Innovative Dynamical Decoupling(DD) Application and Randomized Compiling

Gyunghun Kim,[1] Jongheum Jung,[1] Jungsoo Lee,[1] Seungwon Jung,[1] and Jeongwon Kim[2,*]

[1]*Department of Physics and Astronomy, Seoul National University, Seoul 08826, Korea*

[2]*Sungkyunkwan university, SKKU Advanced Institute of Nano Technology,Dept. of Nano Science and Technology*

(Dated: June 29, 2022)

Randomized benchmarking is one of the most frequently used protocols to benchmark quantum circuits. In the procedure, n-qubit circuits with Clifford gates are constructed. However, constructing multi-qubit circuits with Clifford gates demands tremendous computational power. Fortunately, a former researcher suggested a method that error per Clifford (EPC) of the multi-qubit circuit can be obtained from smaller qubit circuits. Still, there are some differences between this calculated value and the experiment value due to coherent errors in a quantum computer. In this work, we apply dynamical decoupling to mitigate this error and improve error per Clifford of the circuit. By doing that, random benchmarking is executed in a more efficient way, and the difference between the expected EPC value and the experiment value obtained by the IBM backend is reduced. Moreover, we have implemented randomized compilation, another randomizing method for error mitigation in NISQ-era quantum circuits. Applying it on a 4-qubit QFT circuit using a real IBM backend, we have lowered total variational distance (TVD). We provide a visualization of qubit state on different random circuits, and have verified that the randomized compilation method reduces coherent error.

I. INTRODUCTION

II. ERROR MODEL IN RANDOMIZED BENCHMARKING

We perform Randomized Benchmarking(RB) via circuits composed of a series of Clifford circuit layers and the integrated form of each circuit is the same as identity. In real quantum machine, the fidelity follows the equation below.

$$F_{\text{seq}}^{(0}(m, |\psi\rangle) = A_0\alpha^m + B_0, \tag{1}$$

where A0 and B0 are affected by state preparation and measurement errors. We can get the error per Clifford from alpha by $r = \frac{2^n-1}{2^n}(1-\alpha)$. Hence, the error per Clifford can be evaluated if we know α. In general, α also provide us a gate fidelity via Interleaved Randomized Benchmarking(IRB). By interleaving a target gate between every Clifford gate of RB sequence, we can make an IRB sequence. Comparing two results of original RB sequence and IRB sequence, we can retrieve the fidelity of the target gate, since the decaying rate of IRB is decided as that of RB multiplied by the target gate fidelity.

In a high-number qubit system, α is decomposed into low-number qubit system. For instance, α in 3-qubit system, α_{3Q}, satisfies

$$\alpha_{3Q} = \frac{\alpha^{\frac{N_1}{3}}\alpha^{\frac{2N_2}{3}}}{7}(1 + 3\alpha^{\frac{N_1}{3}}\alpha^{\frac{N_2}{3}} + 3\alpha^{\frac{2N_1}{3}}\alpha^{\frac{N_2}{3}}). \tag{2}$$

Here, $N_1(N_2)$ and $\alpha_{1Q}(\alpha_{2Q})$ are the number of single(double)-qubit gates and an alpha value of 1(2) qubit part of the circuit. Still, in real experiment, the result of 3 qubit have had huge differences with the expected value from Eq. (2) due to several coherent errors in circuits.

III. APPLYING DYNAMICAL DECOUPLING TO RB PROCESS

We apply Dynamical Decoupling(DD) to 3 qubit circuits. The inconsistency of Eq. (2) in real experiment can be improved since DD prevents unintended coupling with surroundings by executing pulse sequences that are net-zero to idle qubits. Therefore, we execute XX, XY-4, XY-8, and Uhrig DD sequences to obtain 3-qubit alpha values and compare them with the expected values calculated from Eq. (2) via 1-qubit circuit and 2-qubit circuit during RB.

There are two different DD sequences in a 3 qubit circuit. It can be improved by differing dynamical decoupling with respect to whether the idling qubit is adjacent to the Control(C) qubit or Target(T) qubit. Based on careful verification of the reference through real IBMQ backend, we placed XX sequence when adjacent to C qubit and XYXY sequence (basis gate representation: X-S_X-S_X-$R_Z(\pi)$-X-S_X-S_X-$R_Z(\pi)$) when adjacent to T qubit. We denote these sequences as C sequence and T sequence, respectively.

We implement an algorithm of RB with DD as follows. Owing to differing the DD sequence by the position the sequence is located, we revise the original DD class of Qiskit into our 'MyDynamicalDecoupling' class. This class gets two types of DD sequences and backend information when it is instantiated, and two types of DD sequences are appropriately applied following the topologically ordered directed-acyclic-graph (DAG) of the respective circuit. By saving the recent CNOT gate information as a variable, we can decide which sequence to

* bicycle315

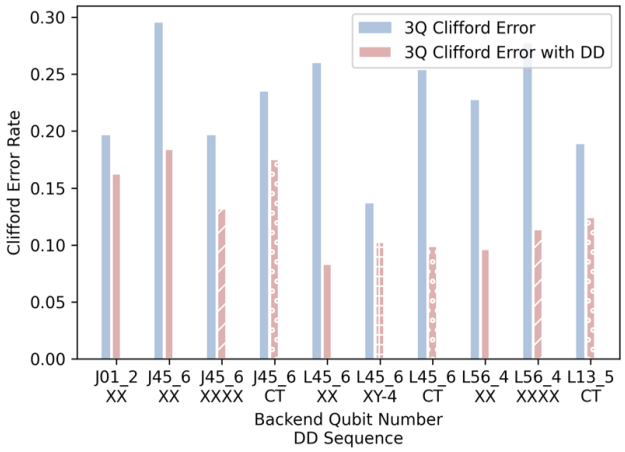

FIG. 1. Cliffored Error Rate measured with and without DD on a variety of qubits in ibmq_jakarta(J) and ibm_lagos(L) backends.

put in each DELAY point of an idling qubit by referring to the connectivity information of the backend. For undecidable cases such as the delay with two CNOT gates being located in the reverse direction as a SWAP gate, T sequence is located as a default. Since some information about overlap is lost when the original circuit is interpreted as DAG, there are also some minor cases which become undecidable due to this interpretation. However, these cases are negligible as the probability of these cases is highly unlikely because the CNOT gate is more than 5 times longer than 1Q gates in duration.

To apply DD in RB, we revised the original Qiskit RB class. Two DD sequences, T sequence, and C sequence, are received as an input when the class is instantiated. Then, two DD sequences are applied using our 'MyDynamicalDecoupling' class and 'PassManager' right after the circuit is transpiled. Interleaved RB is also revised to apply DD by changing the base class to our revised RB class.

IV. DD EFFECT ON RB PROCESS

We retrieved EPC data for diverse backends in IBMQE for 3-qubit RB without and with DD, respectively. As the result in Fig. 1 shows, Clifford error rate was decreased when DD was applied. This verifies our hypothesis that DD would enhance the fidelity of Clifford gates when qubit numbers are bigger than 2, which enables the exponentially decaying curve of RB to decay more slowly.

Fig. 2 shows that Clifford error rate value measured after 3-qubit RB with DD can be expected from simultaneous (2+1)-qubit RB results. Expected Clifford error rate value from simultaneous (2+1)-qubit RB result was calculated according to the equation [**?**]. For diverse qubits on diverse backends, although 3-qubit RB Clifford error rate value without DD has shown a stark difference from the expected value as also shown in the reference, 3-qubit RB Clifford error rate value with DD shows a good correlation with the expected value from (2+1)-qubit RB result. This shows that the unpredictability of 3-qubit RB results was resulted from the presence of idling qubits, which was resolved as DD was implemented to minimize this idling effect.

Fig. 3 shows the implementation of DD with CT sequence on IRB. Firstly, interleaved target gate was generated randomly to be composed of basis gates (X, SX, RZ, and CNOT) as Fig. 3 (a) shows. Number of gates composing the target gate was decided to match its depth equal to that of 3-qubit Clifford gates : 32 1-qubit gates and 8 2-qubit gates. This is due to the fact that, in order to run 3-qubit IRB successfully, we should avoid dilution of target gates that results from its small size compared to intervening Clifford gates. Next, we ran IRB on ibmq-jakarta 0,1,2 qubits for two cases : without DD implementation and with DD implementation using CT sequence, which are shown in Fig. 3 (b) and (c) respectively. The results shows that implementation of DD on IRB slow down the exponential decay of both RB and IRB with higher value of alpha and alpha_c : 0.8133 and 0.9515, respectively, which was increased from 0.7918 and 0.901. Although decay was mostly finished with Clifford length of 10 in without-DD case, decay was postponed to the Clifford length of 13 in with-DD case. And this resulted to a higher accuracy of measured EPC about the respective target gate.

V. RANDOMIZED COMPILATION

Fig. 4 explains what Randomized Compilation(RC) is and demonstrates the objective of RC. The key point of RC is to generate a significant amounts of equivalent circuits to the bare circuit. For each equivalent circuit shown in (a), each output(orange, green, and blue dahsed line) is biased from the ideal outcome due to coherent errors such as over-rotation. However, we can diminish the deviation through RC by taking average value among the equivalent circuits' outputs(gray dotted line). This is because coherent errors are manipulated into a stochastic noise channel due to the combination of the many equivalent circuits' results. In addition, we anticipate that the width of the outcome induced by incoherent errors(e.g., stochastic error) can also be thinner by applying DD sequences. Inserting DD sequences is illustrated in (b) as the timeline representation of a circuit-a timing diagram showing exact pulses executed on a real quantum backend.

To perform RC, many circuits equivalent to the bare circuit are needed. There are two steps to generate multiple circuits. We first follow the conventional method [2, 3]. It has been proposed to twirl gate cycles with a pair of Pauli cycles as a method to generate multiple equivalent circuits with the same depth. A generalized protocol of randomized compilation is deduced as follows. First, determining a set of basis gate and transpile a target cir-

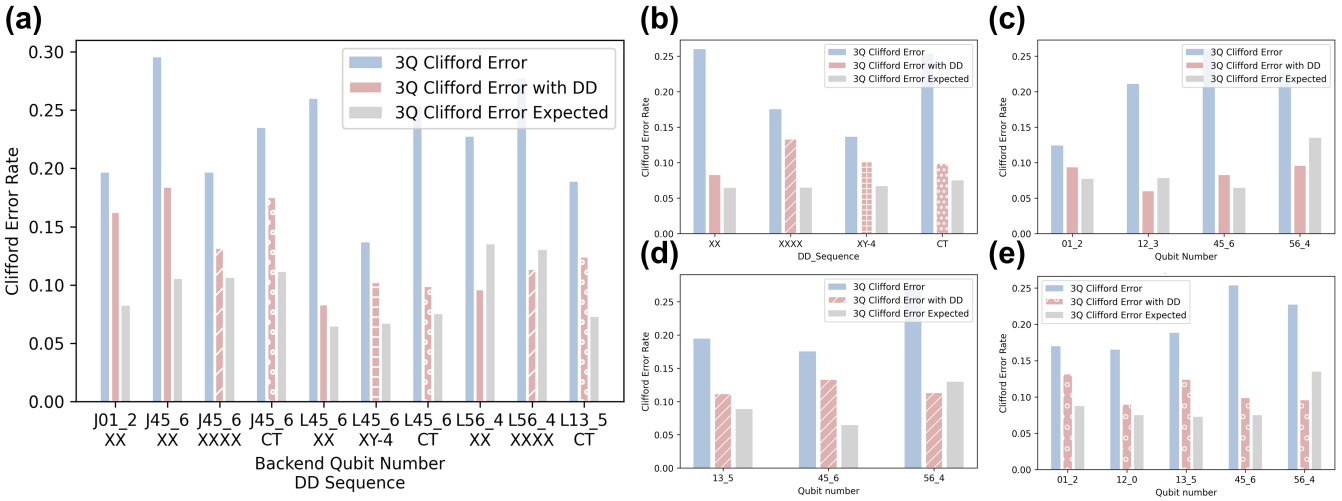

FIG. 2. Clifford Error rate measured for 3-qubit RB, with and without the implementation of DD, and expected value from simultaneous (2+1)-qubit RB.(J for ibmq_jakarta, L for ibm_lagos. Dash lines for XXXX, stripes for XY-4, and bubbles for CT) (a) Accumulative results, and results from (b) Lagos 45_6 qubit, (c) Lagos XX, (d) Lagos XXXX, and (e) Lagos, CT.

cuit using the set only. Subsequently, classifying the basis gates into easy and hard gates. Gate time and error rate are the common criteria. Then randomly twirling easy gate cycle with Pauli gates but keep the net unitary of the circuit intact. To do so, one must conjugate each randomly inserted Pauli cycle with the neighbor hard gate cycle. Finally, recompiling it using the basis gate set. The twirled Pauli cycle including the conjugated ones are included to easy gate cycle.

The second step is to adopt the method on a real IBMQ backend, specifically, on ibmq_jakarta. The overall process is shown in Fig. 6. The basis gate set of the system is RZ,X,S_X,I,C_X. Considering the timing diagram, we classify C_X as the only hard gate. Then we convert all the easy gates into U3 gates. A U_3 gate is universal but costs at most X or S_X gates. A Pauli cycle conjugated by a C_X cycle can always be converted to a U_3 cycle. Therefore, we can obtain another equivalent circuit, with same depth of U_3 and C_X gates. We acknowledge that the depth in terms of the native gates (not U_3) can vary because U_3 gates are implemented either 0, 1, or 2 of gates. However, C_X gates have much longer duration than X or S_X gates. Therefore, the numbers of layers between different generated circuits are effectively equivalent since the number of C_X layers is fixed.

Using the technique, we have conducted an experiment on 4-qubit Qunatum Fourier Transformation(QFT). We have set the initial state to be $|0000\rangle$ and the ideal final state is $|++++\rangle$. The result is summarized in Fig. **??**. We observe substantial improvement using the method.

From (b), state tomography result on our first qubit suggests an explanation to the result. Each point on the Bloch sphere directs away from the ideal $|+\rangle$. However, the averaged arrow, constructed using each point on the sphere, directs much closer to $|+\rangle$, albeit it has a shorter length. It explains the wider but unbiased probability distribution. The QFT applied on the zero state fits to demonstrate this effect.

Finally, (c) shows the number of randomization dependency on Total Variation Distance(TVD). The plot is illustrated in violin plot. The mean value of each number of randomizations is depicted as a black circle, and it exponentially decays(dashed line). Thus, we can verify that RC has a significant effect to reduce the coherence error.

[1] McKay, D. C., Sheldon, S., Smolin, J. A., Chow, J. M., Gambetta, J. M. (2019). Three-qubit randomized benchmarking. Physical review letters, 122(20), 200502.
[2] J. J. Wallman and J. Emerson, Phys. Rev. A **94**, 052325 (2016)
[3] A. Hashim, R. K. Naik, A. Morvan, J. Ville, B. Mitchell, J. M. Kreikebaum, M. Davis, E. Smith, C. Iancu, K. P. O'Brien, I. Hincks, J. J. Wallman, J. Emerson, and I. Siddiqi, Phys. Rev. X **11**, 041039 (2021)

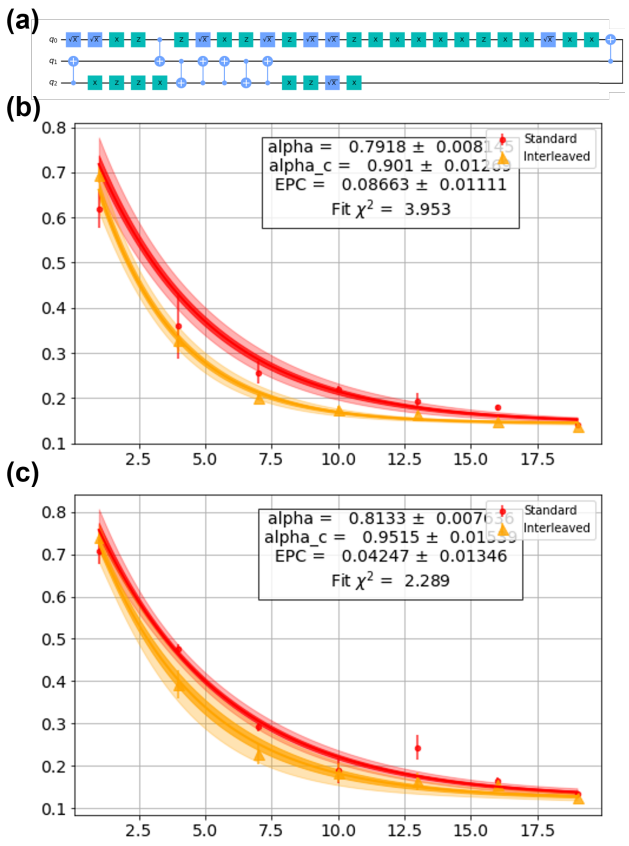

FIG. 3. Interleaved Randomized Benchmarking results about interleaved circuit shown in (a). IRB was conducted without and with the implementation of CT DD sequence, shown in (b) and (c), respectively

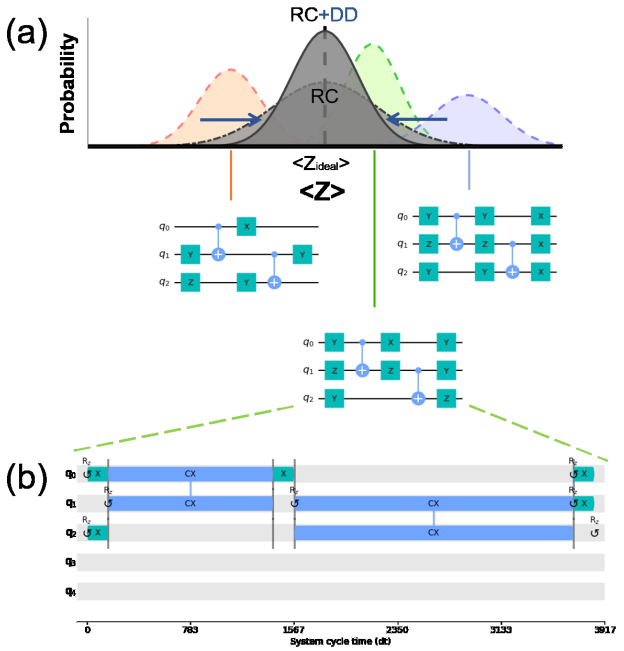

FIG. 4. Explanation of Randomized Compiling(RC) process. We duplicate randomized circuits equivalent from the bare circuit. (a) Output measurement($\langle Z \rangle$) from each randomized circuit. Their values deviate from the ideal circuit due to coherent errors(e.g., over-rotation) and incoherent errors(e.g., depolarizing channel). (b) Timeline illustration for the specific randomized circuit. When applying Dynamical Decoupling(DD), we perform DD sequences to idle qubits in each block.

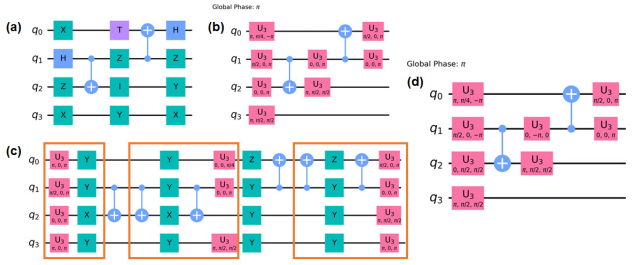

FIG. 5. Generating process of randomized circuits in the IBM backend. (a) An example bare circuit with aligned easy and hard cycles. (b) Easy gates are translated into the U gates. (c) Random Pauli cycles are inserted as well as the conjugated replicas. Groups of cycles that can be merged into easy cycles are grouped by orange boxes. (d) The final circuit of similar depth with the bare one. The easy gates with twirling Paulis are merged into one easy-gate cycle.

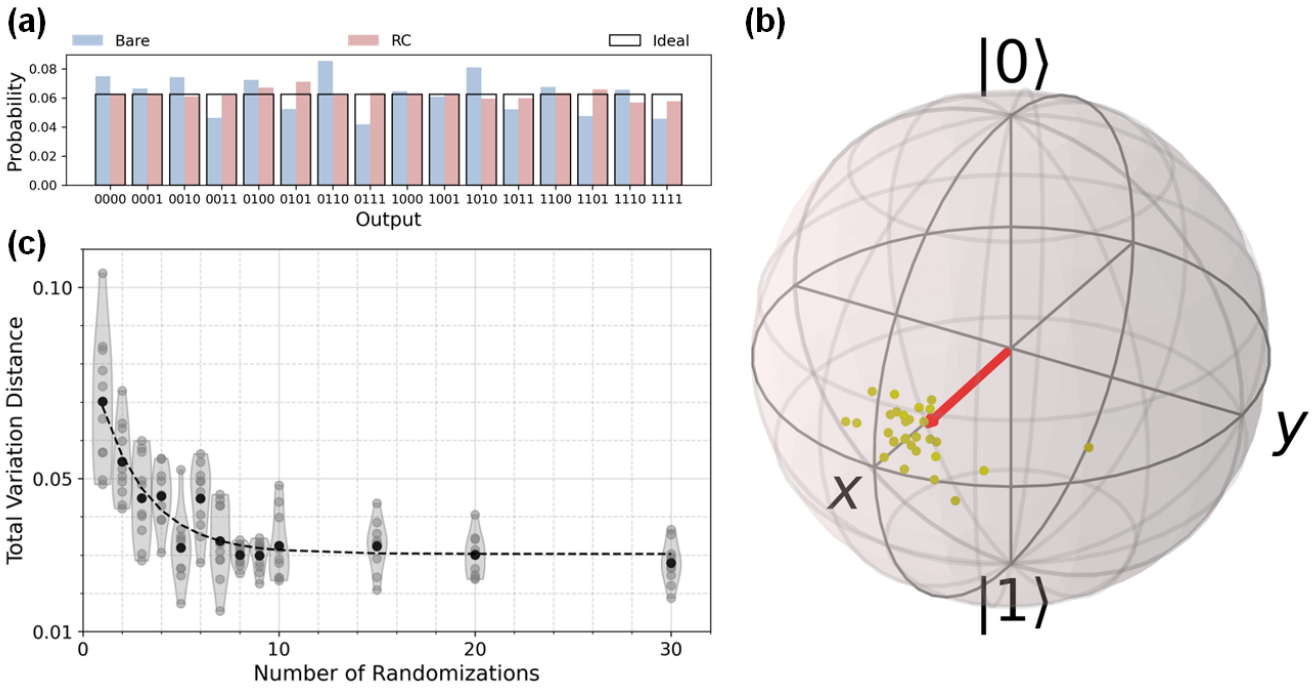

FIG. 6. Experimental result of randomized compiling on 4-qubit quantum Fourier transform circuit. (a) Probability distribution of output when the input is $|0000\rangle$. 30 random circuits are averaged to obtain this result. The ideal result is shown as black contoured boxes. Randomly compiled result is better than the bare circuit. (b) State tomography on the first qubit (q_4 on the real system) of the final states of several randomly compiled and bare circuits. Every circuit has its own bias, but the biases are averaged out to be zero and result in the red arrow. It explains the wider, but unbiased probability density of the method. (c) Plot of TVD versus various number of averaging circuits. Translucent circles indicate all the averaged RC data where the black circles is the mean values of the averaged data with the same number of randomizations. Dashed line shows the exponential fitting curved line of the mean values. The bias decreases exponentially as the number of averaged circuit increases.